Three-dimensional model for human anterior corneal surface

Suilian Zheng
Jinglu Ying
Bo Wang
Zhonghao Xie
Xueping Huang
Mingguang Shi

Three-dimensional model for human anterior corneal surface

Suilian Zheng,[a*] Jinglu Ying,[a,b*] Bo Wang,[c] Zhonghao Xie,[d] Xueping Huang,[d] and Mingguang Shi[a]
[a]The Second Affiliated Hospital of Wenzhou Medical College, Department of Ophthalmology, Wenzhou 325027, China
[b]Zhejiang University, Sir Run Run Shaw Hospital, School of Medicine, Department of Ophthalmology, Hangzhou 310016, China
[c]Nanjing University of Finance and Economics, School of Applied Mathematics, Nanjing 210046, China
[d]Wenzhou Medical College, Department of Computer Science, Wenzhou 325035, China

Abstract. The anterior corneal asphericity (Q) with the tangential radius is calculated, and a three-dimensional (3-D) anterior corneal model is constructed. Tangential power maps from Orbscan II are acquired for 66 young adult subjects. The Q-value of each semimeridian in the near-horizontal region is calculated with the tangential radius. Polynomial fitting is used to model the 360-semimeridional variation of Q-values, and to fit the Q-values in the near-vertical region. Furthermore, a customized 3-D anterior corneal model is constructed. The 360-semimeridional variation of Q-values is well fitted with a seventh-degree polynomial function for all subjects. The goodness of fit of the polynomial function was >0.9, and the median value was 0.94. The Q-value distribution of the anterior corneal surface showed bimodal variation. Additionally, the Q-values gradually become less negative from the horizontal to the vertical semimeridians in the four quadrants. The 3-D surface plot of the anterior corneal surface approximated a prolate ellipsoid. Using a method to calculate the Q-value with the tangential radius combined with polynomial fitting, we are able to obtain the Q-value of any semimeridian. Compared with general models, this method generates a complete shape of the anterior corneal surface using asphericity. © *The Authors. Published by SPIE under a Creative Commons Attribution 3.0 Unported License. Distribution or reproduction of this work in whole or in part requires full attribution of the original publication, including its DOI.* [DOI: 10.1117/1.JBO.18.6.065002]

Keywords: tangential radius of curvature; mathematical model; corneal asphericity; topography.

Paper 12737R received Nov. 15, 2012; revised manuscript received Mar. 26, 2013; accepted for publication May 20, 2013; published online Jun. 24, 2013.

1 Introduction

The anterior surface of the human cornea is a major refractive element. A sound understanding of the corneal shape is needed for the design of the rigid gas permeable (RGP) contact lens and corneal laser refractive surgery (LASIK). Several mathematical models have been proposed to describe the anterior corneal shape.[1–4] In particular, asphericity is an important parameter of the corneal shape that is widely used by corneal topographers.

Guillon et al.[1] and Bennett[5] assumed that the human cornea had a conic section describable by Baker's equation: $y^2 = 2r_0x - px^2$, where p represents the corneal asphericity.[6] Bennett and Rabbetts[7] derived the conic equation, $r_s^2 = r_0^2 + (1 - p)y^2$, to calculate the asphericity by the sagittal radius of curvature (r_s) from keratometry. However, although Bennett's equation is widely used in the studies of corneal shape,[8–12] the sagittal radius of curvature is spherically biased and is not a true radius of curvature.[13–15] Other researchers have described the corneal shape by using the least-squares fitting of zernike polynomials to the data from the corneal height (elevation) map.[16] Recently, Laliberté et al.[17] proposed a method to construct a three-dimensional (3-D) average human corneal model using the data from the elevation map from Orbscan II.

Most previous studies have reported that Q-values are representative of all or two principal corneal meridians. Dubbelman et al.[18] measured the k-values (where $k = Q + 1$) of six semimeridians (0 deg, 30 deg, 60 deg, 90 deg, 120 deg, and 150 deg) using Scheimpflug photography and modeled the meridional variation of the k-values using the $\cos^2$ function. However, the results indicated that the $\cos^2$ function was not an adequate model to describe the variation.

Corneal topography is commonly presented as an axial (sagittal) power, tangential power, or elevation map. The tangential radius of curvature (r_t) is a true radius of curvature that can better represent the corneal shape and local curvature changes.[19] However, to the best of our knowledge, no study has calculated corneal asphericity with the tangential radius of curvature from the tangential power map.

In this study, we calculated the Q-values of the semimeridian based on the tangential radius of curvature using linear regression. For the first time, we elucidated the 360-semimeridional variation rule of the Q-value using the polynomial fitting and constructed a customized 3-D model of the anterior corneal surface. Our mathematical model could be useful in the back-surface fitting of the RGP lens or Q-value-guided customized LASIK.

2 Methods

2.1 Subjects

The right eyes of 66 healthy, young adult volunteers (25 females, 41 males; mean age 24 years; range 18 to 36 years) were evaluated in this study. Inclusion criteria were: (1) refractive spherical equivalent to > -0.25 diopter sphere (DS) and $< +0.50$ DS, (2) corneal astigmatism <1.00 diopter cylinder,

---

*Suilian Zheng and Jinglu Ying contributed equally to the study and were co-first authors.
†This manuscript was presented at the 6th International Conference on Bioinformatics and Biomedical Engineering (ICBBE 2012, Shanghai, China).

Address all correspondence to: Mingguang Shi, The Second Affiliated Hospital of Wenzhou Medical College, Department of Ophthalmology, No. 109, West-Xueyuan Road, Wenzhou 325027, China. Tel: +0086-577-88879100; Fax: +0086-577-88879100; E-mail: pshimg2010@hotmail.com

and (3) absence of detectable ocular disease or history of ocular surgery.

2.2 Data Acquisition

The Bausch & Lomb Orbscan II corneal topographer (version 3.00) was used to acquire topographic images of the right eye of each subject. Three images were obtained from each subject. Topographic images, in which ≥75% of the data were available, were selected for further analysis. The tangential radius of curvature (r_t), the perpendicular distance from the point to the optical axis (y) of all data points on a semimeridian, and the vertex radius of curvature (r_0-value) were obtained from the raw data of the tangential power map of the anterior corneal surface. The data points were arranged on a semimeridian at 0.1-mm intervals. The interval between two semimeridians was 1 deg.

2.3 Q-Value Calculation by Tangential Radius of Curvature

A 3-D Cartesian coordinate system was set with its origin (O) at the vertex normal to the corneal intersection of the optic axis of the corneal topographer.[20] The Z-, Y-, and X-axes of the coordinate system represent the optical axis, vertical, and horizontal directions, respectively. θ was the angle between the corneal meridian section and the XOZ plane. Our published paper[21] has introduced the derivation of the equation in detail for the Q-value calculation by tangential radius. The equation of the corneal meridian section of any angle θ could be expressed as

$$r_t = \frac{1}{r_0^2}[r_0^2 - Qy^2]^{3/2}, \tag{1}$$

where r_t, r_0, Q, and y refer to the tangential radius of curvature, vertex radius of curvature, corneal asphericity, and perpendicular distance from the point to the optical axis, respectively.

As r_t was a nonlinear function of y in Eq. (1), it was difficult to calculate the Q-value. To transform the nonlinear problem into a linear one, Eq. (1) was converted into the form $y^2 = b + cr_t^{2/3}$, where b and c were constants. A straight-line graph of y^2 (on the ordinate) versus $r_t^{2/3}$ (on the abscissa) was plotted. Using linear regression, we obtained $b = (r_0^2/Q)$ and $c = -(r_0^{4/3}/Q)$; that is, $Q = -(b^2/c^3)$. The straight line gives the coefficient of determination (R^2). Considering the reliability of the linear regression equation, the coefficient of determination (R^2) should be >0.5. The Q-value of a given semimeridian was calculated from the first point at 0.1 mm to the peripheral point. The mean of three Q-values of a given semimeridian was regarded as the final value.

2.4 Modeling the 360-Semimeridional Variation Rule of the Q-Value

We previously found that the near-horizontal region showed a good coefficient of determination (R^2), whereas the coefficient of determination for the near-vertical region was relatively poor. This difference between the coefficients of determination may have been due to problems associated with acquiring a good image or because the eyelids induced a nonconic form on the corneal meridian section. Thus, in our previous studies, we were unable to obtain the Q-values of the near-vertical region.

In the present study, according to the Q-value of each semi-meridian in the near-horizontal regions, including 0 deg to 50 deg, 130 deg to 180 deg, 181 deg to 230 deg, and 310 deg to 359 deg, the 360-semimeridional variation of the Q-values for each subject was modeled by polynomial fitting with MATLAB (MathWorks, Inc., Natick, Massachusetts). Then, we fitted the Q-value of each semimeridian in the near-vertical regions, including 51 deg to 129 deg and 231 deg to 309 deg. The polynomial function took the form $f(x) = p_0 + p_1x + p_2x^2 + p_3x^3 + p_4x^4 + \ldots$, where x is the semimeridian angle θ (deg) and $f(x)$ is the corresponding Q-value. The degree was converted to a radian when we performed the polynomial fitting.

3 Construction of a 3-D Model of Corneal Shape

3.1 Rotation of the Coordinate System

A new coordinate system ($\bar{X}O\bar{Y}$) was obtained by rotating the original coordinate system (XOY) counter-clockwise by θ deg (Fig. 1). P was an arbitrary point in the coordinate system, with $P(x, y)$ in the original and $P(\bar{x}, \bar{y})$ in the new coordinate systems, respectively. We obtained the following coordinate rotation formula:

$$\begin{cases} \bar{x} = y \sin \theta + x \cos \theta \\ \bar{y} = y \cos \theta - x \sin \theta \end{cases}. \tag{2}$$

3.2 Generation of a 3-D Corneal Model

We set the angle between a given corneal meridian section and the XOZ plane to be θ deg. A new coordinate system ($\bar{X}O\bar{Y}$) was obtained by rotating the original coordinate system (XOY) around the Z-axis counterclockwise by $-(90 \deg -\theta)$ deg. Thus, the $\bar{Y}OZ$ plane coincided with the corneal meridian section in the new coordinate system ($\bar{X}O\bar{Y}$). The equations of the corneal meridian section in the new coordinate system ($\bar{X}O\bar{Y}$) were as follows:

$$\begin{cases} \bar{x} = 0 \\ \bar{y}^2 = a_1z + a_2z^2 = 2r_0z - (1+Q)z^2 \end{cases}, \tag{3}$$

where ($\bar{x}, \bar{y}$) are the coordinates of the new coordinate system ($\bar{X}O\bar{Y}$). By substituting $-(90 \deg -\theta)$ into θ in Eq. (2), we obtained the following coordinate rotation equations of our corneal model:
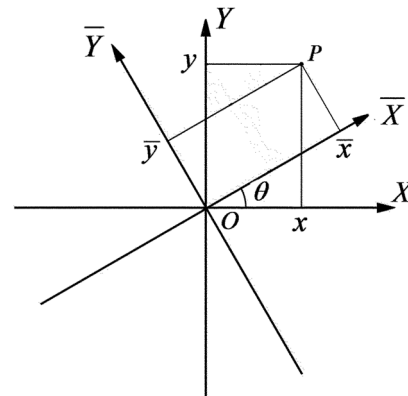

Fig. 1 Schematic diagram of the rotation of the coordinate system.

$$\begin{cases} \bar{x} = x \sin\theta - y \cos\theta \\ \bar{y} = y \sin\theta + x \cos\theta \end{cases}. \qquad (4)$$

We substituted $\bar{x}$, $\bar{y}$ in Eq. (3) to Eq. (4). The equations of the corneal meridian section in the original coordinate system (XOY) were as follows:

$$\begin{cases} x \sin\theta - y \cos\theta = 0 \\ (y \sin\theta + x \cos\theta)^2 = 2r_0 z - (1+Q)z^2 \end{cases}. \qquad (5)$$

Finally, we transformed Eq. (5) into the following form:

$$\begin{cases} x = \sqrt{2r_0 z - (1+Q)z^2}\, \cos\theta \\ y = \sqrt{2r_0 z - (1+Q)z^2}\, \sin\theta \end{cases}, \qquad (6)$$

where θ is any semimeridian angle (deg) and z is a parameter in the equation group.

A total of 360-semimeridians were chosen, and each point had (x, y, z) coordinates. The z-value of each semimeridian was selected from 0 to 3.5 mm at 0.1-mm intervals. The x and y coordinate value of every point was calculated by substituting the corresponding z-value into Eq. (6). Finally, a 3-D corneal surface plot was generated with the Visual C++ 6.0 program.[22]

4 Results

The Kolmogorov–Smirnov test showed that the parameter distributions were not significantly different from normal, except for the goodness of fit (r^2) of the polynomial function.

4.1 Function Relationship

The peripheral points of the semimeridians in the near-horizontal region deviated from the corneal center by up to 4 mm. Figure 2 shows the function scatterplot of the perpendicular distance squared (y^2) versus the tangential radius of curvature to the two-thirds power ($r_t^{2/3}$) on the nasal horizontal principal semimeridian of the right eye for subject number 1. The coefficient of determination (R^2) in the near-horizontal region of most of the right eyes was >0.85.
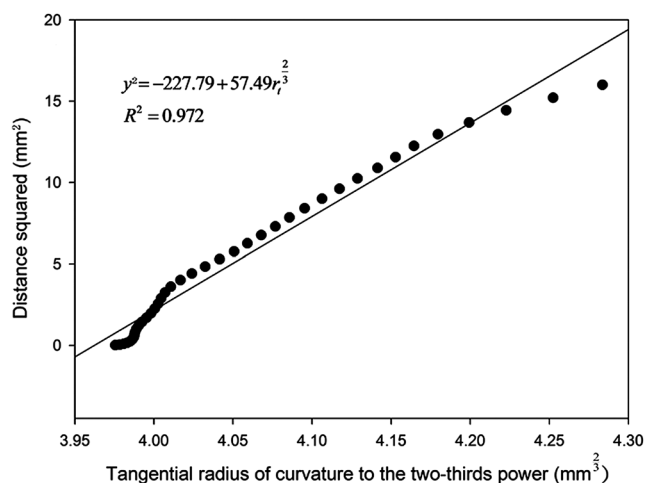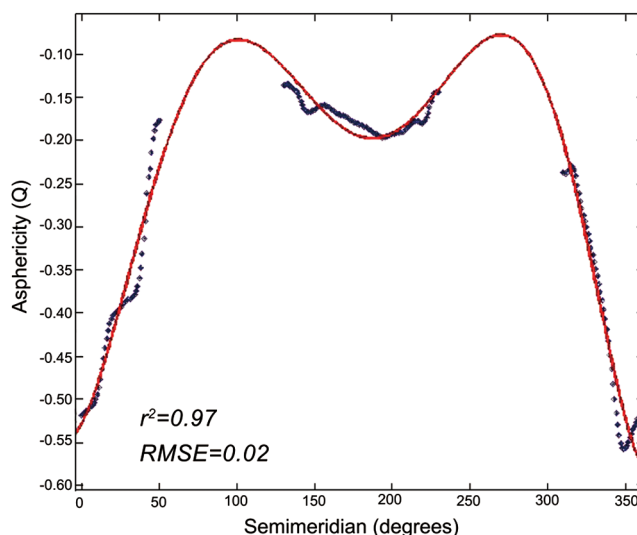
Fig. 2 Scatterplot of perpendicular distance squared (y^2) versus tangential radius of curvature to the two-thirds power ($r_t^{\frac{2}{3}}$) on the nasal horizontal principal semimeridian of the right eye for subject number 1.

Fig. 3 Typical example of the variation of the asphericity (Q) as a function of semimeridian for subject number 22. Blue: Q-value of each semimeridian in the near-horizontal region. Red: Fitted curve of 360-semimeridional variation of the Q-value. r^2: Goodness of fit of the polynomial function. RMSE: RMS fit error.

4.2 360-Semimeridional Variation Rule of the Q-Value

To determine which degree of polynomial would provide an optimal fit to the 360-semimeridional variation of the Q-value, we calculated the root mean square error (RMSE) of the fit of the polynomial function from the fifth to ninth degrees. The RMSE was relatively stable at approximately 0.02 for fits higher than the sixth degree. The 360-semimeridional variation of the Q-value was well fitted with a seventh-degree polynomial function for all subjects.

Figure 3 shows an example of the variation of the asphericity (Q) as a function of the semimeridian for subject number 22 with the following seventh-degree polynomial function:

$$\begin{aligned} f(x) = {} & -0.528 + 0.1977x + 0.3934x^2 - 0.3198x^3 \\ & + 0.06382x^4 + 0.004282x^5 - 0.002427x^6 \\ & + 0.0001822x^7. \end{aligned}$$

Most right eyes displayed a good fit ($r^2 > 0.9$) for the asphericity of all subjects (Fig. 4). The median value was 0.94, and the mean RMSE was 0.02 ± 0.008.

Table 1 shows the mean values of Q at different semimeridian regions in the four quadrants of the anterior corneal surface. The Q-values for the sample analyzed in our study displayed negative values ($-1 < Q < 0$), which gradually became less negative as one moved from the horizontal to the vertical semimeridian regions in each quadrant. Figure 5 shows the variation in asphericity with the semimeridian region of the anterior corneal surface for all subjects. The Q-value distribution of the anterior corneal surface presented bimodal variation with the two peak values representing the least-negative Q-values. The 360-semimeridional variation of Q-values in subjects in Fig. 3 were similar to that of the subjects in Fig. 5.
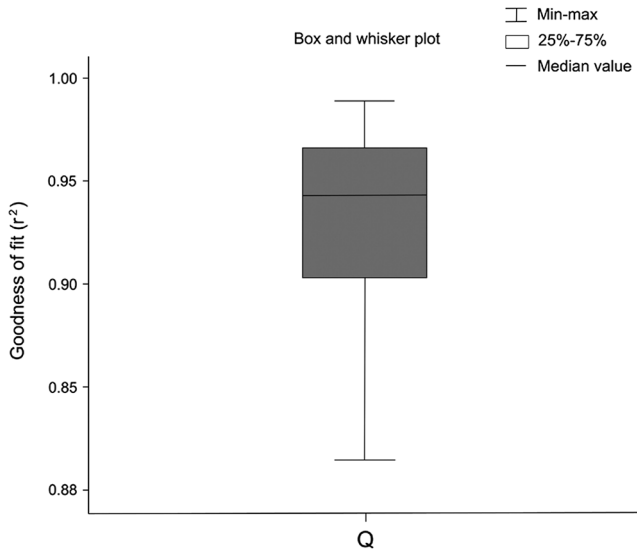
Fig. 4 Box and whisker plot for the goodness of fit (r^2) of the polynomial function for the right eyes of all subjects for the asphericity (Q).
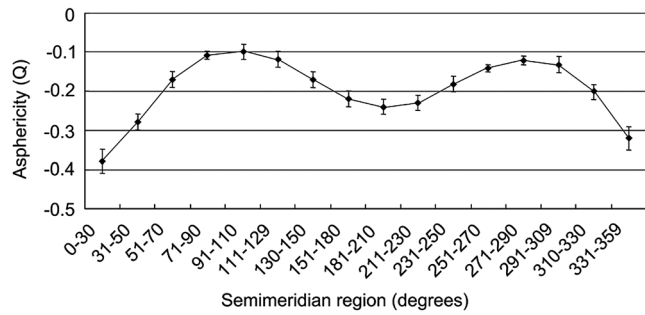

Fig. 5 Variation in asphericity as a function of the semimeridian region of the anterior corneal surface for all subjects. Bars denote 95% confidence interval (CI).

4.3 3-D Corneal Model

Figure 6 shows a colorized 3-D surface plot of the anterior corneal surface described by asphericity (Q) from the different perspectives of the same subject in Fig. 3. The color variation reflects the semimeridional variation of the Q-value with 0.02 color steps. The Q-value gradually becomes more negative from the top to the bottom of the color scale. Because the Q-value of each semimeridian was a negative value ($-1 < Q < 0$) corresponding to the most common corneal shape,[23] the 3-D surface plot of the anterior corneal surface approximated a prolate ellipsoid.

5 Discussion

Douthwaite et al.[24] used linear regression to calculate Q-values with the sagittal radius of curvature (r_s) according to Bennett's equation $r_s^2 = r_0^2 + (1 - p)y^2$. There are two differences between Q-values calculated using the sagittal or tangential radius of curvature. First, because the sagittal radius of curvature (r_s) is spherically biased, it is not a true radius of curvature. The tangential radius of curvature (r_t) is a true radius of curvature

that better represents corneal shape and local curvature changes. Second, Bennett's equation does not include rotation of the coordinate system. Therefore, it can only be used to calculate Q-values of the principal semimeridians or principal semiaxes. Although the Q-value calculation of our method was more complex, it could calculate Q-values of the four principal semiaxes as well as those of other semimeridians. Current corneal topographers provide Q-values that are representative of all or the two principal corneal meridians. We modeled the 360-semimeridional variation of the Q-value, which was well fitted with a seventh-degree polynomial function for all subjects.

Laliberte et al.[17] proposed a method for constructing an average 3-D human corneal model based on elevation data from Orbscan II. They used the best-fit sphere (BFS) as a reference surface. The colorized anterior elevation map showed that the elevation with respect to the BFS (green) was slightly positive (yellow-red) in the central region. Additionally, a mid-peripheral yellow-green pattern was located above the BFS.

In our study, we proposed a method for constructing a customized 3-D human corneal model by asphericity based on the tangential radius of curvature. Figure 6 shows a typical 3-D surface plot of the anterior corneal surface, which was approximated as a prolate ellipsoid. The corneal curvature gradually became flatter from the center toward the periphery. Q-values in the near-vertical region were less negative (warmer colors) than those in the near-horizontal region, and those in the nasal cornea were more negative (colder colors) than those in the temporal cornea. A corneal model constructed from elevation

Table 1 Values for asphericity (Q) at different semimeridian regions in four quadrants of the anterior corneal surface.

$n = 66$	Corneal semimeridian region (deg)							
	0 to 30	31 to 50	51 to 70	71 to 90	91 to 110	111 to 129	130 to 150	151 to 180
Mean± SD	-0.38 ± 0.13	-0.28 ± 0.10	-0.18 ± 0.07	-0.12 ± 0.06	-0.10 ± 0.07	-0.12 ± 0.08	-0.17 ± 0.10	-0.22 ± 0.10
Range	-0.72 to -0.10	-0.61 to -0.07	-0.42 to -0.06	-0.29 to -0.01	-0.31 to 0.01	-0.44 to -0.01	-0.55 to -0.04	-0.54 to -0.06
$n = 66$	181 to 210	211 to 230	231 to 250	251 to 270	271 to 290	291 to 309	310 to 330	331 to 359
Mean± SD	-0.24 ± 0.11	-0.23 ± 0.09	-0.18 ± 0.07	-0.14 ± 0.06	-0.12 ± 0.05	-0.14 ± 0.06	-0.20 ± 0.09	-0.32 ± 0.13
Range	-0.56 to -0.05	-0.47 to -0.03	-0.36 to -0.02	-0.30 to -0.02	-0.27 to -0.02	-0.29 to -0.03	-0.45 to -0.05	-0.70 to -0.07

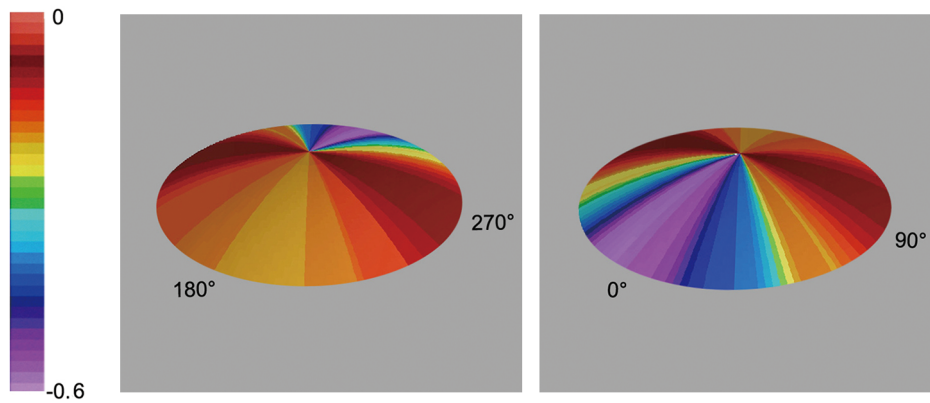Note: n = number of eyes; SD = standard deviation.

Fig. 6 Three-dimensional (3-D) surface plot of anterior corneal surface described by asphericity (Q) for the same subject as in Fig. 2. Color scale (left) represents variation of the Q-value.

data does not have a specific mathematical equation to describe the corneal shape and cannot describe the corneal asphericity (Q). Instead, such a model shows the elevation difference at each point on the corneal surface from the BFS. In contrast, we constructed a corneal model that was quantitatively described by asphericity.

Anterior corneal asphericity is an important parameter for back-surface fitting of the RGP lens and for Q-value-guided customized LASIK. The goal of the aspheric back-surface RGP lens design is to optimize alignment with the anterior corneal surface. The goal of the Q-value-guided customized LASIK is to maintain the physiological asphericity of the anterior corneal surface. At present, Q-values of the two principal meridians or the four principal semimeridians are used to guide RGP lens fitting and LASIK design. Our mathematical model improves on previous methods by providing 360 Q-values of the semimeridians of the whole anterior corneal surface.

In conclusion, we have proposed a method to calculate the anterior corneal asphericity (Q) of the semimeridian using the tangential radius of curvature (r_t). Furthermore, our study provided 360 Q-values of semimeridians of the whole anterior corneal surface, and we constructed a customized 3-D corneal model that was completely described by asphericity. Our mathematical model could help to optimize the back-surface fitting of the RGP lens or Q-value-guided customized LASIK, thereby improving a patient's visual quality.

Acknowledgments

References

1. M. Guillon, D. P. M. Lydon, and C. Wilson, "Corneal topography: a clinical model," *Ophthal. Physiol. Opt.* **6**(1), 47–56 (1986).
2. W. Lotmar, "Theoretical eye model with asphercis," *J. Opt. Soc. Am.* **61**(11), 1522–1529 (1971).
3. R. B. Mandel, "The enigma of corneal contour: Everett Kinsey lecture," *CLAO J.* **18**(4), 267–273 (1992).
4. R. Lindsay, G. Smith, and D. Atichson, "Descriptors of corneal shape," *Optom. Vis. Sci.* **75**(2), 156–158 (1998).
5. A. G. Bennett, "Aspherical and continuous curve contact lenses," *Optom. Today* **28**(1), 11–14; **28**(5), 140–142; **28**(9), 238–242; **28**(16), 433–444 (1988).
6. T. Y. Baker, "Ray tracing through non-spherical surfaces," *Proc. Phys. Soc.* **55**(5), 361–364 (1943).
7. A. G. Bennett and R. B. Rabbetts, "What radius does the conventional keratometer measure?," *Ophthal. Physiol. Opt.* **11**(3), 239–247 (1991).
8. S. W. Cheung, P. Cho, and W. A. Douthwaite, "Corneal shape of Hong Kong-Chinese," *Ophthalmic Physiol. Opt.* **20**(2), 119–125 (2000).
9. W. A. Douthwaite and W. T. Evardson, "Corneal topography by keratometry," *Br. J. Ophthalmol.* **84**(8), 842–847 (2000).
10. W. A. Douthwaite, "The asphericity, curvature and tilt of the human cornea measured using a video keratoscope," *Ophthalmic Physiol. Opt.* **23**(2), 141–150 (2003).
11. W. R. Davis et al., "Corneal asphericity and apical curvature in children: a cross-sectional and longitudinal evaluation," *Invest. Ophthalmol. Vis. Sci.* **46**(6), 1899–1906 (2005).
12. W. A. Douthwaite and E. A. Mallen, "Cornea measurement comparison with Orbscan II and EyeSys video keratoscope," *Optom. Vis. Sci.* **84**(7), 598–604 (2007).
13. C. Roberts, "Characterization of the inherent error in a spherically-biased corneal topography system in mapping a radially aspheric surface," *J. Refract Corneal. Surg.* **10**(2), 103–111 (1994).
14. C. Roberts, "Analysis of the inherent error of the TMS-1 Topographic Modeling System in mapping a radially aspheric surface," *Cornea* **14**(3), 258–265 (1995).
15. J. S. Chan et al., "Accuracy of video keratography for instantaneous radius in keratoconus," *Optom. Vis. Sci.* **72**(11), 793–799 (1995).
16. D. R. Iskander, M. J. Collins, and B. Davis, "Optimal modeling of corneal surfaces with Zernike polynomials," *IEEE Trans. Biomed. Eng.* **48**(1), 87–95 (2001).
17. J. F. Laliberté et al., "Construction of a 3-D atlas of corneal shape," *Invest. Ophthalmol. Vis. Sci.* **48**(3), 1072–1078 (2007).
18. M. Dubbelman, V. A. Sicam, and G. L. Van der Heijde, "The shape of the anterior and posterior surface of the aging human cornea," *Vision Res.* **46**(6–7), 993–1001 (2006).
19. L. B. Szczotka and J. Thomas, "Comparison of axial and instantaneous video keratographic data in keratoconus and utility in contact lens curvature prediction," *CLAO J.* **24**(1), 22–28 (1998).
20. R. B. Mandell, C. S. Chiang, and S. A. Klein, "Location of the major corneal reference points," *Optom. Vis. Sci.* **72**(11), 776–784 (1995).
21. J. Ying, B. Wang, and M. Shi, "Anterior corneal asphericity calculated by the tangential radius of curvature," *J. Biomed. Opt.* **17**(7), 075005 (2012).
22. J. D. Foley et al., *Computer Graphics: Principles and Practice in C*, 2nd ed., Addison-Wesley, Boston (1995).
23. P.M. Kiely, G. Smith, and L. G. Carney, "The mean shape of the human cornea," *Opt. Acta* **29**(8), 1027–1040 (1982).
24. W. A. Douthwaite, "EyeSys corneal topography measurement applied to calibrated ellipsoidal convex surfaces," *Br. J. Ophthalmol.* **79**(9), 797–801 (1995).